

# Mechanically-driven spreading of bacterial population

Waipot Ngamsaad<sup>a,\*</sup>, Suthep Suantai<sup>b</sup>

<sup>a</sup>*Division of Physics, School of Science, University of Phayao, Phayao 56000, Thailand*

<sup>b</sup>*Department of Mathematics, Faculty of Science, Chiang Mai University, Chiang Mai 50200, Thailand*

---

## Abstract

The effect of mechanical interaction between cells on the spreading of bacterial population was investigated in one-dimensional space. A continuum mechanical approach, comprising cell migration, proliferation and exclusion process, has been employed to elucidate this dynamics. The consequent nonlinear reaction-diffusion-like equation arises as the constitution of the bacterial population dynamics. In this model, the bacterial cells are treated as the rod-like particles that interact, when contacting each other, through the hard-core repulsion. The repulsion introduces the exclusion effect that causes the bacterial populations to migrate fast at high density. The propagation of the bacterial density as the traveling wave front in long time behavior has been analyzed. The analytical and numerical solutions reveal that the front speed is enhanced by the exclusion process, which depends on the cell packing fraction. The qualitative comparison between the theoretical results and the experimental evidences is discussed.

*Keywords:* Traveling wave, Nonlinear reaction-diffusion model, Bacterial colony

---

## 1. Introduction

In past decades, much attention has paid to the collective behaviors of bacterial populations. This system is used as the prototype for understanding the multicellular assemblies such as tissue and biofilm [1]. The insight into the underlying mechanism of dynamics is important to biological and medical science.

To cope with unflavored environmental conditions, the bacterial colonies generate the varieties of pattern formations [2, 3]. The spatiotemporal pattern formation in bacterial colonies is resulted from the migration and proliferation of cells. This dynamics at continuum level can be described by the reaction-diffusion processes [2–4]. The simplified model [2] relied on the density-dependent (or degenerate) reaction-diffusion equation [5–9], which is the exten-

---

\*Corresponding author

Email addresses: [waipot.ng@up.ac.th](mailto:waipot.ng@up.ac.th) (Waipot Ngamsaad), [scmti005@chiangmai.ac.th](mailto:scmti005@chiangmai.ac.th) (Suthep Suantai)

sion of the classical Fisher-KPP equation [10, 11]. The well-known exact solutions [7, 8] revealed that the bacterial density evolves as the sharp traveling wave with constant front speed [2]. In our previous work, we found an explicit space-time solution of the generalized Fisher-KPP equation, in one-dimensional space [12]. This solution evolves, from a specific initial condition, as a self-similar object that converges to the usual traveling wave on a long-time scale. Although it can explain this dynamics, the conventional model has omitted the size of the bacterial cell. In real systems, the most of bacterial cells have rod shape and grow in dense environments. Accordingly, the mechanical interaction between cells could play the crucial roles on the spreading of bacterial colony.

The recent experimental and theoretical studies have shown that the mechanical interaction between cells has important roles on the collective behaviors of the bacterial colonies [13–18]. The dependence on the elastic modulus of the front speed has been found in theory [19]. It has mentioned that *the migration of the bacteria is caused by cell pushing rather than self-propelling* in dense colony [14, 17, 18]. Therefore, we speculate that the exclusion process, that prevents overlapping of cells, could play the crucial roles on the spreading of bacterial colony. This issue motivates us to extend the conventional density-dependent reaction-diffusion equation [5–9] by incorporating with the cell size for investigating the dynamics of bacterial population.

In this work, we consider the systems of bacterial cells that are growing on the thin layer of nutrient-contained fluid medium. The bacteria increase population numbers by cell division and interact each other through the hard-core repulsion (steric interaction); which causes the exclusion effect and consequent non-overlap of cells. Although the bacteria are self-propelled particles [20], in the colony of densely packed or nonmotile cells, the migration of the bacteria is caused by cell pushing, arises from cell growth and division, rather than self-propelling [14, 17, 18]. Thus, *the bacteria behave as, more or less the same, passive particles or nonmotile cells* in high density. Apart from cells, Bruna and Chapman [21] analyzed that the self-diffusion of the hard-spherical Brownian particles, in dilute regime, decreases with increasing density; because the diffusion of any single particle is impeded by the collisions with others particle. But, the collisions bias the particle to move towards the low density regions, by which the biased migration is faster than the self-diffusion. So that, the overall effective collective diffusion is enhanced. As guided by the work of Bruna and Chapman [21], we propose that the bacterial cells are moved by the purely hard-core repulsion without self-motion in dense colony.

When incorporating with the exclusion processes in cell (or particle) dynamics, the altered diffusion coefficients in the continuum limits have been found [22–29]. The enhancement or slowing down of diffusion depends on the cell length and the allowed moving distance, as shown by the lattice-based analysis [28]. Crucially, in some models, the diffusion diverges to infinity at the close-packed density [22, 23, 29]. The singular diffusion has been also modeled the migration of bacterial biofilm [30, 31] and glioblastoma tumor [32]. However, how the diverged diffusion affects the propagation speed of cell populations is unrevealed.

To address this question, this research employs the continuum mechanical approach with cell proliferation [33] to investigate the spreading of the bacterial populations in the presence of the exclusion process. The front speed of bacterial colony expansion in the term of cell size parameter is provided both analytically and numerically. The consistency of our theoretical results with the experimental evidences is discussed.

## 2. Continuum mechanical model

### 2.1. Constitution equations

In macroscopic view point, the bacterial populations are the continuum fluid that can reproduce to increase cell numbers. By pushing each other away after cell division [14, 17, 18], the population pressure arises due to the collisions between cells and drives the cells to move. When moving, the cells face with the friction from the surrounding fluid medium and the substrate surface. For the sake of simplicity, we consider the expansion of bacterial colonies in one-dimensional space, regardless of cell orientation effect. Adapting from Ref. [33], the constitution equations, that describe the evolution of the number density  $\rho(x, t)$  and the collective velocity  $V(x, t)$  of the bacterial population at position  $x$  and time  $t$ , are given by

$$\frac{\partial \rho}{\partial t} = -\frac{\partial(\rho V)}{\partial x} + \Gamma(\rho), \quad (1)$$

$$-\gamma V = \frac{\partial p}{\partial x} = \frac{\partial p}{\partial \rho} \frac{\partial \rho}{\partial x}, \quad (2)$$

where  $p(\rho(x, t))$  is the internal population pressure and  $\gamma$  is damped constant. Eq. (1) is continuity equation with the growth term  $\Gamma(\rho)$ . As usual, we assume that the growth of bacteria obeys the logistic law:  $\Gamma(\rho) = k\rho(1 - \rho/\rho_m)$ , where  $k$  is rate constant and  $\rho_m$  is the maximum density [9, 33]. Eq. (2) arises from the force balance between Stokes' friction and the pressure gradient—and it is similar to the Darcy's law that describes the fluid flow in porous media.

We model the bacterial cells as the non-overlap hard-rod particles with the average length  $\sigma$  that interact through the hard-core repulsion. In high density, the self-propulsion of bacteria can be ignored since it is dominated by the collision between cells. This turns the bacterial cell to be the passive particle or nonmotile cell, more or less the same, that obeys the usual thermodynamic laws. For the hard-rod fluid in one dimension, the exact pressure is known

$$p(\rho) = \frac{\rho k_B T}{1 - \sigma \rho}, \quad (3)$$

where  $k_B$  is Boltzmann constant and  $T$  is temperature [34–36]. In our case that the bacterial cells behave as the passive particles, the temperature relates to the average translation kinetic energy of a cell—that  $\langle E_k \rangle = (1/2)k_B T$ . We assume that the temperature is constant in our system. The pressure in Eq. (3)

diverges to infinity at the close-packed density:  $\rho \rightarrow 1/\sigma$ . Notably, in dilute density,  $\rho \rightarrow 0$ , Eq. (3) recovers the pressure of an ideal gas:  $p = \rho k_B T$ . As pointed out in Refs. [37–39], the pressure for dilute active particle is similar to the ideal gas. Except that, the source of kinetic energy comes from the swim speed  $U_0$ :  $k_B T \sim U_0^2$  [37, 38]. It will be seen later that the specific source of temperature is not important; as long as it is constant, the dynamics of our model is invariant.

## 2.2. Dimensionless equations

We define the maximum density as  $\rho_m = 1/\sigma_m$  where  $\sigma_m$  is the average length occupied by one cell and  $\sigma_m > \sigma > 0$ . The logistic law limits the growth of bacteria such that  $0 \leq \rho \leq \rho_m < 1/\sigma$ . For convenience in further analysis, we introduce the dimensionless quantities:  $0 \leq u = \rho/\rho_m \leq 1$ ,  $v = [\gamma/(k\rho_m k_B T)]^{1/2} V$ ,  $0 < \epsilon = \sigma\rho_m = \sigma/\sigma_m < 1$ ,  $t' = \alpha t$  and  $x' = [(k\gamma)/(k\rho_m k_B T)]^{1/2} x$ . In one dimension, the packing fraction ( $\epsilon$ ) means the length fraction and it is equivalent to the area and volume fraction in two and three dimensions, respectively. Then, we rewrite Eq. (1) and Eq. (2) by employing Eq. (3) in dimensionless form

$$\frac{\partial u}{\partial t} = -\frac{\partial(uv)}{\partial x} + u(1-u), \quad (4)$$

$$v = -\frac{1}{(1-\epsilon u)^2} \frac{\partial u}{\partial x}, \quad (5)$$

where the prime has been dropped. From Eq. (5), the migration of bacterial populations is biased to move downwards density gradient and is enhanced by the exclusion process, implying from the factor  $1/(1-\epsilon u)^2$ . It increases with density and diverges to infinity as  $\epsilon \rightarrow 1$  at  $u = 1$ —that cause the bacterial population to migrate very fast at high density. The singularity has also appeared in the similar models by different approaches [22, 23, 29–32, 40]. Fortunately, the velocity in Eq. (5) should be finite since  $\partial u/\partial x \rightarrow 0$  at  $u = 1$ . The fact is that the density inside the colony reaches the saturated value except in the vicinity of colony edge. At this point, the density distribution is homogeneous and its gradient approaches zero.

Substituting Eq. (5) into Eq. (4), we obtain a nonlinear partial differential equation

$$\frac{\partial u}{\partial t} = \frac{\partial}{\partial x} \left( M(u) \frac{\partial u}{\partial x} \right) + g(u), \quad (6)$$

where  $M(u) = u/(1-\epsilon u)^2$  and  $g(u) = u(1-u)$ . Eq. (6) is exactly in the same form of the density dependent reaction-diffusion equation—but the migration coefficient is different from the diffusive one. It obviously does not relate to the mean square displacement but  $M \sim \rho \partial p / \partial \rho$ . Because, in this model, the populations are migrated by the collision between cells rather than the random walk. The similar coefficient represents the contribution of hard-core repulsion between cells to the migration of myxobacteria in dense phase [40]. Eq. (6)

is degenerate in the sense that  $M(0) = 0$ , which results the sharp interface, separated between occupied and cell-free region. In very dilute system ( $\epsilon \rightarrow 0$ ), Eq. (6) recovers the conventional degenerate Fisher-KPP equation [7–9]; in which the explicit solution has been found in our previous work [12].

### 3. Traveling wave solution

We focus on long time behavior of the system that the population density propagates as the traveling wave:  $u(x, t) = \phi(z)$ , where  $z = x - ct$  and  $c$  is the front speed [9]. Substituting the traveling wave solution into Eq. (6), we obtain

$$\frac{d}{dz} \left( M(\phi) \frac{d\phi}{dz} \right) + c \frac{d\phi}{dz} + g(\phi) = 0. \quad (7)$$

In the degenerate model, the density must vanish at the finite position  $z^* (< \infty)$  that undergoes the sharp interface. Then, we consider the density profile that satisfies the following conditions:  $\phi(-\infty) = 1$ ,  $\phi(z) = 0$  for  $z \geq z^*$ ,  $\frac{d}{dz}\phi(-\infty) = 0$ , and  $\frac{d}{dz}\phi(z^*) \neq 0$ . In addition, for  $\epsilon \in [0, 1)$ ,  $M(\phi(-\infty)) < \infty$  and  $M(\phi(z)) = 0$  for  $z \geq z^*$  [41]. Multiplying Eq. (7) by  $M(\phi)d\phi/dz$  and then integrating with respect to  $z$  from  $-\infty$  to  $z^*$ , we obtain  $c \int_{-\infty}^{z^*} M(\phi) \left( \frac{d\phi}{dz} \right)^2 dz + \int_{-\infty}^{z^*} M(\phi) g(\phi) \frac{d\phi}{dz} dz + \frac{1}{2} \left( M(\phi) \frac{d\phi}{dz} \right)^2 \Big|_{-\infty}^{z^*} = 0$ . With the density profile conditions, the last term is zero and finally we obtain the front speed

$$c = - \frac{\int_0^1 M(\phi) g(\phi) d\phi}{\int_0^1 M(\phi) \left( \frac{d\phi}{dz} \right) d\phi}. \quad (8)$$

To obtain the closed-form of the front speed  $c$ , it requires solution of the density gradient  $d\phi/dz$ .

#### 3.1. Approximate solution

Although the exact solution of Eq. (7) has been unknown, we can find the approximate solution by employing the perturbation method as used in Ref. [42]. By defining  $w(\phi) = d\phi/dz$ , we rewrite Eq. (7)

$$M(\phi) w \frac{dw}{d\phi} + M'(\phi) w^2 + cw + g(\phi) = 0, \quad (9)$$

where  $M'(\phi) = dM(\phi)/d\phi$ . The migration coefficient can be written in the expansion form:  $M(\phi) \approx \phi (1 + 2\phi\epsilon + 3\phi^2\epsilon^2 + \dots)$ . We then look for the solution of Eq. (9) in the power series of  $\epsilon$

$$w(\phi) = w_0(\phi) + w_1(\phi)\epsilon + w_2(\phi)\epsilon^2 + \dots, \quad (10)$$

$$c = c_0 + c_1\epsilon + c_2\epsilon^2 + \dots, \quad (11)$$

where  $w_i(\phi)$  and  $c_i$ , that  $i \in \{0, 1, 2, \dots, \infty\}$ , are coefficients to be determined. Substituting Eq. (10) and Eq. (11) into Eq. (9), we obtain the equation for each order as follows: at  $\epsilon^0$ ,

$$\phi w_0 \frac{dw_0}{d\phi} + w_0^2 + c_0 w_0 + \phi(1 - \phi) = 0, \quad (12)$$

and, at  $\epsilon^1$ ,

$$\begin{aligned} \phi w_0 \frac{dw_1}{d\phi} + \left( \phi \frac{dw_0}{d\phi} + 2w_0 + c_0 \right) w_1 \\ + 2\phi^2 w_0 \frac{dw_0}{d\phi} + 4\phi w_0^2 + c_1 w_0 = 0. \end{aligned} \quad (13)$$

Eq. (12) has the known solutions:  $w_0 = (1/\sqrt{2})(\phi - 1)$  and  $c_0 = 1/\sqrt{2}$  [7–9, 42]. Substituting these solutions into Eq. (13), we obtain a linear first order ordinary differential equation

$$\begin{aligned} \phi(\phi - 1) \frac{dw_1}{d\phi} + (3\phi - 1) w_1 \\ + 3\sqrt{2}\phi^3 - 5\sqrt{2}\phi^2 + (2\sqrt{2} + c_1)\phi - c_1 = 0. \end{aligned} \quad (14)$$

After finding the integrating factor [43], we obtain its solution

$$\begin{aligned} w_1(\phi) = \frac{1}{(\phi - 1)^2} \left[ \frac{C}{\phi} - \frac{3\sqrt{2}}{5}\phi^4 + 2\sqrt{2}\phi^3 \right. \\ \left. - \left( \frac{c_1}{3} + \frac{7\sqrt{2}}{3} \right) \phi^2 + \left( c_1 + \sqrt{2} \right) \phi - c_1 \right], \end{aligned} \quad (15)$$

where  $C$  is integral constant. To prevent the singularity at  $\phi = 0$  and  $\phi = 1$ , we require that  $C = 0$  and  $-\frac{3\sqrt{2}}{5} + 2\sqrt{2} - \left( \frac{c_1}{3} + \frac{7\sqrt{2}}{3} \right) + (c_1 + \sqrt{2}) - c_1 = 0$ . Thus we obtain

$$c_1 = \frac{2}{5\sqrt{2}}. \quad (16)$$

Substituting Eq. (16) into Eq. (15), after doing some algebra, we obtain

$$w_1(\phi) = -\frac{2}{5\sqrt{2}}(\phi - 1)(3\phi - 1). \quad (17)$$

Finally, gathering all terms, we obtain the approximate solutions to the correction of  $O(\epsilon^2)$

$$w = \frac{d\phi}{dz} = \frac{6(\phi - 1)}{5\sqrt{2}} \left( \frac{5 + 2\epsilon}{6} - \epsilon\phi \right) + O(\epsilon^2), \quad (18)$$

$$c = \frac{1}{\sqrt{2}} \left( 1 + \frac{2}{5}\epsilon \right) + O(\epsilon^2). \quad (19)$$

The density gradient approaches zero when the density reaches its maximum,  $\phi \rightarrow 1$ , as expected. By using  $w(\phi) = d\phi/dz$ , we can calculate the approximate density profile

$$\phi(z) = \begin{cases} \frac{1-\exp[b(z-z_0)]}{1-a\exp[b(z-z_0)]}, & z \leq z_0 \\ 0, & z > z_0, \end{cases} \quad (20)$$

where  $a = \frac{6\epsilon}{5+2\epsilon}$ ,  $b = \frac{5-4\epsilon}{5\sqrt{2}}$  and  $z_0$  is the initial front position that  $\phi(z_0) = 0$ .

### 3.2. Front speed

The front speed is the collective velocity at the edge of colony,  $c = v(\phi(z^*)) = v(0)$ . To the correction of  $O(\epsilon^2)$ , from Eq. (19), the front speed increases linearly with packing fraction ( $\epsilon$ ). However, substituting Eq. (18) into Eq. (8), after integrating, we can obtain more precise front speed

$$c(\epsilon) = \frac{5}{\sqrt{2}\epsilon} \frac{(4\epsilon - 6) \ln(1 - \epsilon) + \epsilon^2 - 6\epsilon}{(2\epsilon^2 - 11\epsilon + 8) \ln(1 - \epsilon) - 7\epsilon^2 + 8\epsilon}. \quad (21)$$

It has found that the front speed depends on the packing fraction of cell. It recovers the usual value, that  $c_0 = 1/\sqrt{2} \approx 0.7071$ , in very dilute regime, as  $\epsilon \rightarrow 0$ , [7–9, 42]). At the close-packed value, as  $\epsilon \rightarrow 1$ , the front speed approaches a finite value that  $c(1) = 10/\sqrt{2} \approx 7.071$ . It increases by a factor of 10 from the dilute regime.

## 4. Numerical results and discussion

As the correction of our approximate solutions is limited to  $O(\epsilon^2)$ , it is counter-intuitive—since the model is designed for capturing the dynamics at high density. To obtain the actual results at high density, we solved Eq. (6), subjected to the zero flux boundary condition, directly by using the numerical method. In Eq. (6), the migration coefficient increases with density. It is inefficient by solving with the explicit finite difference scheme [44]. Unfortunately, solving with the standard implicit numerical scheme is also difficult because the factor  $1/(1 - \epsilon u)^2$ . We have found that the simplest algorithm that overcomes these obstructions is the nonstandard fully implicit finite difference method as used in Ref. [30]. It has been proved that this algorithm is stable enough to explore the dynamics with high packing fraction. The detailed algorithm is described in the Appendix.

In our computation, we choose the spacing step and the time step, respectively, such that  $\delta x = 0.25$  and  $\delta t = 0.05$ . The computations are performed on 10,000 grids with 10,000 iterations. The initial density profile,  $u_0(x)$ , is set to a step function

$$u_0(x) = \begin{cases} 1, & x < r_0 \\ 0, & x \geq r_0, \end{cases} \quad (22)$$

where  $r_0$  is initial front position. Here, we choose that  $r_0 = 500$ , to ensure that it is far enough from the boundary at origin. The front position  $r_f(t)$  is the

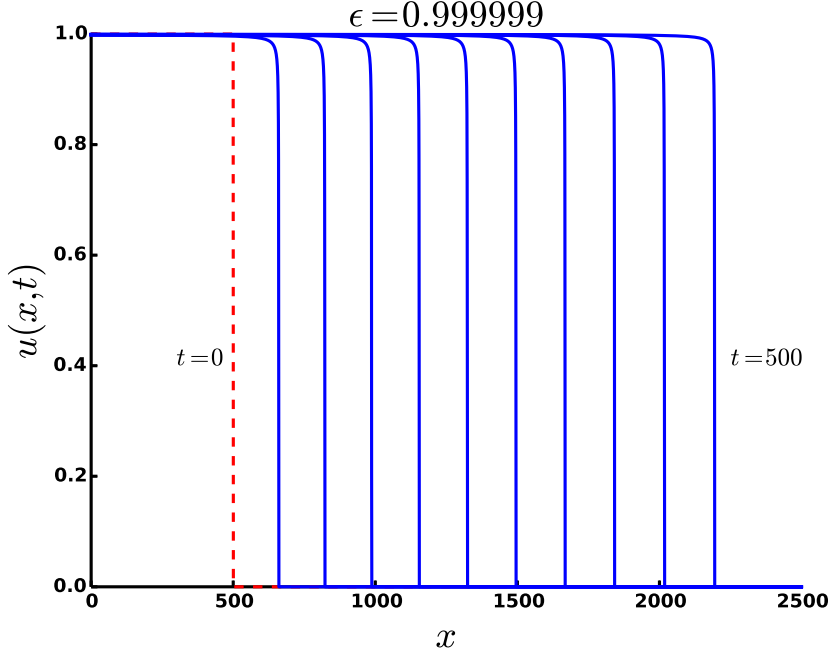


Figure 1: (Color online) The demonstration of density profile,  $u(x, t)$ , that is obtained by using the numerical method for  $\epsilon = 0.999999$  from  $t = 0$  to  $t = 500$ . The dashed line is initial density profile. The data are shown for every  $t = 50$ .

first position that the density falls to zero. Technically, due to the numerical deviation, we measure the first position that the density is less than or equal to  $1 \times 10^{-6}$ —or  $u(r_f, t) \leq 1 \times 10^{-6}$ . The front positions are collected for every  $t = 5$ . The last 50 data points are selected for fitting with the linear equation,  $r_f = ct + r_0$ , to avoid the transient effect of initial stage. Hence, the slope of this linear equation is equal to the front speed.

First, we tested the accuracy of our algorithm by calculating the front speed for  $\epsilon = 0$ . In this case, the numerical front speed is equal to 0.7156, which shows the error about 0.8% of the exact value ( $c_0 = 1/\sqrt{2} \approx 0.7071$  [7–9, 42]). We then study the dynamics of bacterial population at close-packed regime. In the computation, we set  $\epsilon = 0.999999$ , to avoid the dividing by zero of the factor  $1/(1-\epsilon u)^2$  when  $u = 1$ . The demonstration of the density profile, obtained from the numerical method, is shown in Fig. (1) for  $\epsilon = 0.999999$ . It is observed that the density profile evolves as the sharp traveling wave with unchanged shape. The front position, in a function of time, is well fitted with the linear equation as shown in Fig. (2). It implies that the density propagates with constant front speed, which is equal to the slope of linear equation. Very closed to the close-packed value,  $\epsilon = 0.999999$ , the numerical front speed is equal to 3.4831, which is less than the analytical predicted value due to the inaccuracy of the

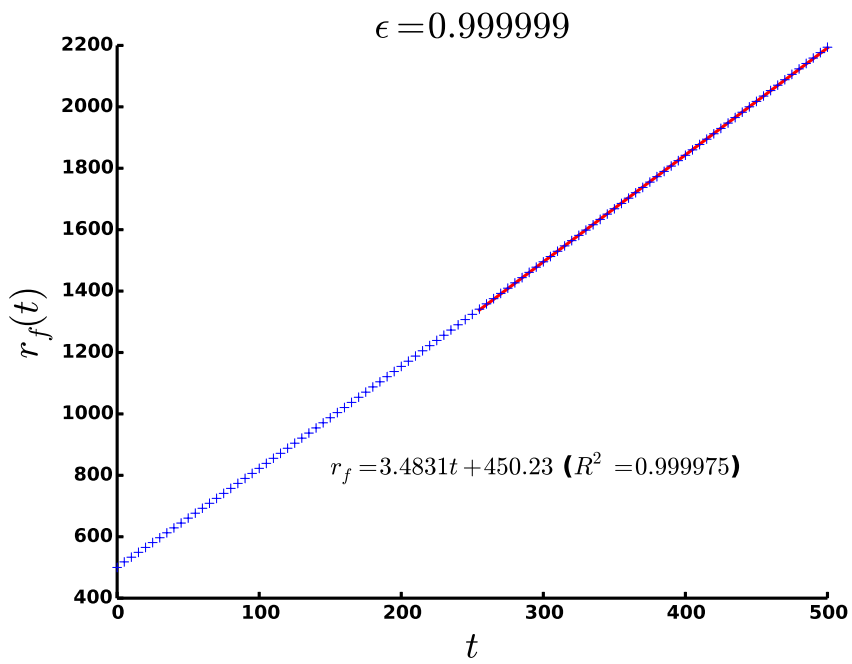


Figure 2: (Color online) The demonstration of the front position versus time of numerical density profile for  $\epsilon = 0.999999$  from  $t = 0$  to  $t = 500$ . The data are shown for every  $t = 5$ . The markers are numerical values and the solid linear is the fitting linear equation for the last 50 data points.  $R^2$  is the correlation coefficient.

approximate solution.

Although our model is not expected to be accurate for dilute system since it has neglected the self-propulsion of bacteria, we attempt to compare our theoretical results to the experimental evidences. In our numerical data, the front speed at the close-packed regime increases by a factor of  $\sim 5$  from the dilute regime. This is in qualitatively agreement with the experimental observations where the dependence on the packing fraction of the average (or typical) velocity of bacterial suspensions has been found [45, 46]. At the close-packed density, the increase of the average velocity by a factor of  $\sim 3$  found in the suspensions of the spherical-shaped bacteria [46] and the increase of the typical velocity by a factor of  $\sim 5$  found in the suspensions of the rod-shaped bacteria [45]. The different is that the decay of velocity above the close-packed density cannot be observed in our results—since the close-packed fraction for one-dimensional hard-rod system is equal to 1.

## 5. Conclusion

This theoretical study has demonstrated the effect of mechanical interaction between cells on the spreading of the bacterial populations by employing a continuum approach modeling. In dense colony, the migration of the bacteria is dominated by the hard-core repulsion between cells that causes the exclusion process. The analytical and numerical results reveal that the expansion speed of bacterial colony is enhanced by the exclusion effect, which depends on the cell packing fraction. This prediction is consistent with the experimental evidences, at least in qualitatively.

## Acknowledgment

This research was supported by the TRF Grant for New Researcher (No. TRG5780037) funded by The Thailand Research Fund and University of Phayao.

## Appendix A. Nonstandard fully implicit finite difference scheme

We define the discrete density as  $u_j^n = u(x_j, t_n)$  where  $x_j = j\delta x$ ,  $t_n = n\delta t$ ,  $\delta x$  is spacing step,  $\delta t$  is time step,  $j \in \{0, 1, 2, \dots, J\}$ ,  $n \in \{0, 1, 2, \dots, N\}$ , and  $J$  and  $N$  are integer. Then, we rewrite Eq. (6)

$$\frac{\partial u_j^{n+1}}{\partial t} \approx \frac{\partial}{\partial x} \left( M_j^n \frac{\partial u_j^{n+1}}{\partial x} \right) + f_j^n u_j^{n+1}, \quad (\text{A.1})$$

where  $M_j^n = M(u_j^n) = u_j^n / (1 - \epsilon u_j^n)^2$  and  $f_j^n = 1 - u_j^n$ . Using the standard discretized scheme for the differential operators, we obtain

$$\begin{aligned} \frac{u_j^{n+1} - u_j^n}{\delta t} &= \frac{1}{\delta x} \left( M_{j+1/2}^n \frac{\partial}{\partial x} u_{j+1/2}^{n+1} \right. \\ &\quad \left. - M_{j-1/2}^n \frac{\partial}{\partial x} u_{j-1/2}^{n+1} \right) + f_j^n u_j^{n+1}. \end{aligned} \quad (\text{A.2})$$

We discretize further for the remain gradient terms in Eq. (A.2) and then we have

$$\begin{aligned} \frac{u_j^{n+1} - u_j^n}{\delta t} &= \frac{1}{(\delta x)^2} \left[ M_{j+1/2}^n (u_{j+1}^{n+1} - u_j^{n+1}) \right. \\ &\quad \left. - M_{j-1/2}^n (u_j^{n+1} - u_{j-1}^{n+1}) \right] + f_j^n u_j^{n+1}. \end{aligned} \quad (\text{A.3})$$

The migration coefficient at the mid-grid can be computed by

$$M_{j-1/2}^n = \frac{1}{2} (M_{j-1}^n + M_j^n), \quad (\text{A.4})$$

$$M_{j+1/2}^n = \frac{1}{2} (M_j^n + M_{j+1}^n). \quad (\text{A.5})$$

Noting that the correction of Eq. (A.3) is  $O(\delta t, (\delta x)^2)$ . After rearranging Eq. (A.3), we have

$$\alpha_j^n u_{j-1}^{n+1} + \theta_j^n u_j^{n+1} + \beta_j^n u_{j+1}^{n+1} = u_j^n, \quad (\text{A.6})$$

where

$$\begin{aligned} \alpha_j^n &= -\mu M_{j-1/2}^n, \\ \beta_j^n &= -\mu M_{j+1/2}^n, \\ \theta_j^n &= 1 - \delta t f_j^n + \mu (M_{j-1/2}^n + M_{j+1/2}^n), \\ \mu &= \delta t / (\delta x)^2. \end{aligned} \quad (\text{A.7})$$

We impose the zero flux condition at the boundary grid, saying  $\Omega$ , that  $\frac{\partial u}{\partial x}|_{\Omega} = 0$  or  $\frac{u_{\Omega+1}^n - u_{\Omega-1}^n}{2\delta x} = 0$ . Consequently,  $u_{\Omega-1}^n = u_{\Omega+1}^n$  and  $M_{\Omega-1/2}^n = M_{\Omega+1/2}^n$ . Then, we rewrite Eq. (A.6), subjected to the zero flux boundary condition, in the matrix form

$$\mathbf{A}^n \cdot \mathbf{U}^{n+1} = \mathbf{U}^n, \quad (\text{A.8})$$

where

$$\mathbf{A}^n = \begin{bmatrix} \theta_0^n & 2\beta_0^n & \cdots & \cdots & 0 \\ \alpha_1^n & \theta_1^n & \beta_1^n & & \vdots \\ \vdots & \ddots & \ddots & \ddots & \vdots \\ \vdots & & \alpha_{J-1}^n & \theta_{J-1}^n & \beta_{J-1}^n \\ 0 & \cdots & \cdots & 2\alpha_J^n & \theta_J^n \end{bmatrix}, \quad (\text{A.9})$$

and

$$\mathbf{U}^n = [u_0^n \ u_1^n \ u_2^n \ \cdots \ u_J^n]^T. \quad (\text{A.10})$$

According to the boundary condition,  $\theta_0^n = 1 - \delta t f_0^n + 2\mu M_{1/2}^n$  and  $\theta_J^n = 1 - \delta t f_J^n + 2\mu M_{J-1/2}^n$ . The numerical density can be obtained by solving the matrix equation (Eq. (A.8)) iteratively.

To find the stability condition of this numerical scheme, we use the von Neumann solution

$$u_j^n = (\lambda)^n e^{ikj\delta x}, \quad (\text{A.11})$$

where  $\lambda$  is amplification factor and  $k$  is wave number [44]. Substituting Eq. (A.11) into Eq. (A.3), we obtain  $\lambda^{-1} = 1 - \delta t f_j^n - \mu M_{j+1/2}^n (e^{ik\delta x} - 1) + \mu M_{j-1/2}^n (1 - e^{-ik\delta x})$ , which it can be approximated further

$$\lambda \approx [1 - \delta t f_j^n + 4\mu M_j^n \sin^2(k\delta x/2) + O(\delta x)]^{-1}. \quad (\text{A.12})$$

For stable and temporal non-oscillated numerical solution, it requires that  $0 < \lambda \leq 1$  [30]. According to the fact that  $0 \leq f_j^n \leq 1$  and  $0 \leq M_j^n < \infty$ , without the growth term ( $f_j^n$ ), this algorithm is unconditional stable as long as  $\delta x \ll 1$  [44]. With the growth term, solution slowly grows to the finite value as long as  $\delta t \ll 1$ . As proved in Eq. (A.12), this algorithm is quite stable for this kind of problem.

## References

- [1] Shapiro JA. Thinking about bacterial populations as multicellular organisms. *Annu Rev Microbiol* 1998;52(1):81–104. doi:10.1146/annurev.micro.52.1.81.
- [2] Kawasaki K, Mochizuki A, Matsushita M, Umeda T, Shigesada N. Modeling spatio-temporal patterns generated by bacillus subtilis. *J Theor Biol* 1997;188(2):177–85.
- [3] Ben-Jacob E, Cohen I, Levine H. Cooperative self-organization of microorganisms. *Adv Phys* 2000;49:395–554.
- [4] Golding I, Kozlovsky Y, Cohen I, Ben-Jacob E. Studies of bacterial branching growth using reaction-diffusion models for colonial development. *Physica A* 1998;260(3-4):510–54.
- [5] Gurney W, Nisbet R. The regulation of inhomogeneous populations. *J Theor Biol* 1975;52(2):441–57.
- [6] Gurtin M, MacCamy R. On the diffusion of biological populations. *Math Biosci* 1977;33(1-2):35–49.
- [7] Newman W. Some exact solutions to a non-linear diffusion problem in population genetics and combustion. *J Theor Biol* 1980;85(2):325–34.
- [8] Newman W. The long-time behavior of the solution to a non-linear diffusion problem in population genetics and combustion. *J Theor Biol* 1983;104(4):473–84.
- [9] Murray J. *Mathematical Biology*. Springer-Verlag, New York; 1989.

- [10] Fisher R. The wave of advance of advantageous genes. *Ann Eugenics* 1937;7(4):355–69.
- [11] Kolmogorov A, Petrovskii I, Piscounov N. A study of the diffusion equation with increase in the amount of substance, and its application to a biological problem. In: Tikhomirov V, editor. *Selected works of AN Kolmogorov*. Springer; 1991, p. 242–70.
- [12] Ngamsaad W, Khompurngson K. Self-similar solutions to a density-dependent reaction-diffusion model. *Phys Rev E* 2012;85:066120.
- [13] Cho H, Jönsson H, Campbell K, Melke P, Williams JW, Jedynak B, et al. Self-organization in high-density bacterial colonies: Efficient crowd control. *PLoS Biol* 2007;5(11):e302. URL: <http://dx.doi.org/10.1371/journal.pbio.0050302>. doi:10.1371/journal.pbio.0050302.
- [14] Volfson D, Cookson S, Hasty J, Tsimring LS. Biomechanical ordering of dense cell populations. *Proc Nat Acad Sci USA* 2008;105(40):15346–51.
- [15] Mather W, Mondragón-Palomino O, Danino T, Hasty J, Tsimring L. Streaming instability in growing cell populations. *Phys Rev Lett* 2010;104:208101. URL: <http://link.aps.org/doi/10.1103/PhysRevLett.104.208101>. doi:10.1103/PhysRevLett.104.208101.
- [16] Boyer D, Mather W, Mondragón-Palomino O, Orozco-Fuentes S, Danino T, Hasty J, et al. Buckling instability in ordered bacterial colonies. *Phys Biol* 2011;8(2):026008. URL: <http://stacks.iop.org/1478-3975/8/i=2/a=026008>.
- [17] Su PT, Liao CT, Roan JR, Wang SH, Chiou A, Syu WJ. Bacterial colony from two-dimensional division to three-dimensional development. *PLoS ONE* 2012;7(11):e48098. URL: <http://dx.doi.org/10.1371/journal.pone.0048098>. doi:10.1371/journal.pone.0048098.
- [18] Grant MAA, Waclaw B, Allen RJ, Cicuta P. The role of mechanical forces in the planar-to-bulk transition in growing escherichia coli microcolonies. *J R Soc Interface* 2014;11(97).
- [19] Farrell F, Hallatschek O, Marenduzzo D, Waclaw B. Mechanically driven growth of quasi-two-dimensional microbial colonies. *Phys Rev Lett* 2013;111(16):168101.
- [20] Cates ME. Diffusive transport without detailed balance in motile bacteria: does microbiology need statistical physics? *Rep Prog Phys* 2012;75(4):042601. URL: <http://stacks.iop.org/0034-4885/75/i=4/a=042601>.

[21] Bruna M, Chapman SJ. Diffusion of multiple species with excluded-volume effects. *J Chem Phys* 2012;137(20):204116. URL: <http://scitation.aip.org/content/aip/journal/jcp/137/20/10.1063/1.4767058>. doi:<http://dx.doi.org/10.1063/1.4767058>.

[22] Bodnar M, Velazquez JJL. Derivation of macroscopic equations for individual cell-based models: a formal approach. *Math Methods Appl Sci* 2005;28(15):1757–79. URL: <http://dx.doi.org/10.1002/mma.638>. doi:[10.1002/mma.638](http://dx.doi.org/10.1002/mma.638).

[23] Lushnikov PM, Chen N, Alber M. Macroscopic dynamics of biological cells interacting via chemotaxis and direct contact. *Phys Rev E* 2008;78:061904. URL: <http://link.aps.org/doi/10.1103/PhysRevE.78.061904>. doi:[10.1103/PhysRevE.78.061904](http://dx.doi.org/10.1103/PhysRevE.78.061904).

[24] Simpson MJ, Baker RE, McCue SW. Models of collective cell spreading with variable cell aspect ratio: A motivation for degenerate diffusion models. *Phys Rev E* 2011;83:021901. URL: <http://link.aps.org/doi/10.1103/PhysRevE.83.021901>. doi:[10.1103/PhysRevE.83.021901](http://dx.doi.org/10.1103/PhysRevE.83.021901).

[25] Baker RE, Simpson MJ. Models of collective cell motion for cell populations with different aspect ratio: Diffusion, proliferation and travelling waves. *Physica A* 2012;391(14):3729 –50. URL: <http://www.sciencedirect.com/science/article/pii/S0378437112000192>. doi:<http://dx.doi.org/10.1016/j.physa.2012.01.009>.

[26] Bruna M, Chapman SJ. Excluded-volume effects in the diffusion of hard spheres. *Phys Rev E* 2012;85:011103. URL: <http://link.aps.org/doi/10.1103/PhysRevE.85.011103>. doi:[10.1103/PhysRevE.85.011103](http://dx.doi.org/10.1103/PhysRevE.85.011103).

[27] Dyson L, Maini PK, Baker RE. Macroscopic limits of individual-based models for motile cell populations with volume exclusion. *Phys Rev E* 2012;86:031903. URL: <http://link.aps.org/doi/10.1103/PhysRevE.86.031903>. doi:[10.1103/PhysRevE.86.031903](http://dx.doi.org/10.1103/PhysRevE.86.031903).

[28] Penington CJ, Hughes BD, Landman KA. Interacting motile agents: Taking a mean-field approach beyond monomers and nearest-neighbor steps. *Phys Rev E* 2014;89:032714. URL: <http://link.aps.org/doi/10.1103/PhysRevE.89.032714>. doi:[10.1103/PhysRevE.89.032714](http://dx.doi.org/10.1103/PhysRevE.89.032714).

[29] Almet AA, Pan M, Hughes BD, Landman KA. When push comes to shove: Exclusion processes with nonlocal consequences. *Physica A* 2015;437(0):119 –29. URL: <http://www.sciencedirect.com/science/article/pii/S037843711500446X>. doi:<http://dx.doi.org/10.1016/j.physa.2015.05.031>.

[30] Eberl HJ, Demaret L. A finite difference scheme for a degenerated diffusion equation arising in microbial ecology. *Electron J Diff Eqns, Conference* 2007;15:77–95.

[31] Jalbert E, Eberl HJ. Numerical computation of sharp travelling waves of a degenerate diffusionreaction equation arising in biofilm modelling. *Commun Nonlinear Sci Numer Simulat* 2014;19(7):2181–90. URL: <http://www.sciencedirect.com/science/article/pii/S1007570413005248>. doi:<http://dx.doi.org/10.1016/j.cnsns.2013.11.001>.

[32] Harko T, Mak MK. Travelling wave solutions of the reaction-diffusion mathematical model of glioblastoma growth: An abel equation based approach. *Math Biosci Eng* 2015;12(1):41–69. URL: <http://aims.science.org/journals/displayArticlesnew.jsp?paperID=10615>. doi:[10.3934/mbe.2015.12.41](http://dx.doi.org/10.3934/mbe.2015.12.41).

[33] Arciero JC, Mi Q, Branca MF, Hackam DJ, Swigon D. Continuum model of collective cell migration in wound healing and colony expansion. *Biophys J* 2011;100(3):535–43.

[34] Tonks L. The complete equation of state of one, two and three-dimensional gases of hard elastic spheres. *Phys Rev* 1936;50:955–63. URL: <http://link.aps.org/doi/10.1103/PhysRev.50.955>. doi:[10.1103/PhysRev.50.955](http://dx.doi.org/10.1103/PhysRev.50.955).

[35] Salsburg ZW, Zwanzig RW, Kirkwood JG. Molecular distribution functions in a onedimensional fluid. *J Chem Phys* 1953;21(6):1098–107. URL: <http://scitation.aip.org/content/aip/journal/jcp/21/6/10.1063/1.1699116>. doi:<http://dx.doi.org/10.1063/1.1699116>.

[36] Helfand E, Frisch HL, Lebowitz JL. Theory of the two and onedimensional rigid sphere fluids. *J Chem Phys* 1961;34(3):1037–42. URL: <http://scitation.aip.org/content/aip/journal/jcp/34/3/10.1063/1.1731629>. doi:<http://dx.doi.org/10.1063/1.1731629>.

[37] Takatori SC, Yan W, Brady JF. Swim pressure: Stress generation in active matter. *Phys Rev Lett* 2014;113:028103. URL: <http://link.aps.org/doi/10.1103/PhysRevLett.113.028103>. doi:[10.1103/PhysRevLett.113.028103](http://dx.doi.org/10.1103/PhysRevLett.113.028103).

[38] Takatori SC, Brady JF. Towards a thermodynamics of active matter. *Phys Rev E* 2015;91:032117. URL: <http://link.aps.org/doi/10.1103/PhysRevE.91.032117>. doi:[10.1103/PhysRevE.91.032117](http://dx.doi.org/10.1103/PhysRevE.91.032117).

[39] Solon AP, Stenhammar J, Wittkowski R, Kardar M, Kafri Y, Cates ME, et al. Pressure and phase equilibria in interacting active brownian spheres. *Phys Rev Lett* 2015;114:198301. URL: <http://link.aps.org/doi/10.1103/PhysRevLett.114.198301>. doi:[10.1103/PhysRevLett.114.198301](http://dx.doi.org/10.1103/PhysRevLett.114.198301).

[40] Harvey CW, Alber M, Tsimring LS, Aranson IS. Continuum modeling of myxobacteria clustering. *New J Phys* 2013;15(3):035029. URL: <http://stacks.iop.org/1367-2630/15/i=3/a=035029>.

[41] Garduño FS, Maini P. Traveling wave phenomena in some degenerate reaction-diffusion equations. *J Differ Equations* 1995;117(2):281 – 319. URL: <http://www.sciencedirect.com/science/article/pii/S0022039685710558>. doi:<http://dx.doi.org/10.1006/jdeq.1995.1055>.

[42] Garduño FS, Maini P. An approximation to a sharp type solution of a density-dependent reaction-diffusion equation. *Appl Math Lett* 1994;7(1):47 – 51. URL: <http://www.sciencedirect.com/science/article/pii/0893965994900515>. doi:[http://dx.doi.org/10.1016/0893-9659\(94\)90051-5](http://dx.doi.org/10.1016/0893-9659(94)90051-5).

[43] Arfken GB. Mathematical Methods for Physicists. Academic Press, San Diego; 1985.

[44] Press WH, Flannery BP, Teukolsky SA, Vetterling WT. Numerical Recipes in C: The Art of Scientific Computing. Cambridge University Press, Cambridge; 1988.

[45] Sokolov A, Aranson IS, Kessler JO, Goldstein RE. Concentration dependence of the collective dynamics of swimming bacteria. *Phys Rev Lett* 2007;98:158102. URL: <http://link.aps.org/doi/10.1103/PhysRevLett.98.158102>. doi:[10.1103/PhysRevLett.98.158102](http://10.1103/PhysRevLett.98.158102).

[46] Rabani A, Ariel G, Be'er A. Collective motion of spherical bacteria. *PLoS ONE* 2013;8(12):e83760. URL: <http://dx.doi.org/10.1371/journal.pone.0083760>. doi:[10.1371/journal.pone.0083760](http://10.1371/journal.pone.0083760).